Optical Materials 42 (2015) 276–280

Contents lists available at ScienceDirect

Optical Materials

journal homepage: www.elsevier.com/locate/optmat

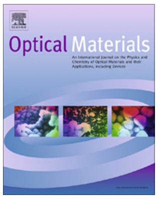

Spectroscopic properties of nonlinear optical $LiGaTe_2$ crystal

A. Yelisseyev [a,*], P. Krinitsin [a], L. Isaenko [a,b], S. Grazhdannikov [a]

[a] *Institute of Geology and Mineralogy, Russian Acad Sci, Siberian Branch, 3 Academician Koptyug Ave, 630090 Novosibirsk, Russia*
[b] *Novosibirsk State University, 2 Pirogova Str., 630090 Novosibirsk Russia*

ARTICLE INFO

Article history:
Received 19 June 2014
Received in revised form 10 November 2014
Accepted 21 December 2014
Available online 2 February 2015

Keywords:
$LiGaTe_2$
Growth
Absorption
Luminescence
Raman scattering

ABSTRACT

The nonlinear crystal $LiGaTe_2$ (LGT) with chalcopyrite structure was grown by the Bridgman–Stockbarger technique. LGT is transparent in the 0.52–16 μm range. Fundamental absorption edge is due to direct allowed transitions; Band gap values are 2.65 and 2.41 eV at 80 and 300 K, respectively. Vibrational, Raman and IR absorption spectra demonstrate four groups of lines in the 50–350 cm^{-1}. Intense orange photoluminescence (PL) in a broad 605 nm band, excited at band-to-band transitions and quenched in the 180–250 K range is related to self-trapped excitons. Weaker PL components at 510, 729 and 898 nm are associated supposedly with F-centers and their complexes. According to PL excitation spectra valence band is split into three components: Γ_7(A), Γ_6(B) and Γ_7(C), from which electrons are excited to the bottom of the conduction band Γ_6. The crystal field splitting (Δ_{CF}) and the spin–orbit splitting (Δ_{SO}) were determined to be −0.75, and 0.62 respectively, at liquid nitrogen temperature.

1. Introduction

The compound $LiGaTe_2$ (LGT) was mentioned for the first time in relation to possible tetragonal structures of the chalcopyrite type in the family of the $Li^{I}Me^{III}X_2^{VI}$ chalcogenides [1] where Me^{III} = Al, Ga, In, and X^{VI} = S, Se, Te. On the basis of the so-called electronegativity differences the authors, who determined the space group $I\bar{4}2d$ or D_{2d}^{12}, No. 122 of LiInTe (LIT), predicted the same chalcopyrite ($CuFeS_2$) structure for LGT [1]. The existence of LGT was also predicted in a more general systematics of the $Li^{I}Me^{III}X_2$ ^{VI}-type compounds where Me^{III} = Ga, In, Tl and X^{VI} = S, Se, Te [2] and melting temperature of 1002 K and a band-gap of 1.7 eV were predicted for LGT [2]. The first LGT crystals, grown by the Tammann–Stöber technique, were black in color and did not exhibit a single phase, decomposing within hours into small-grained LGT, GaTe and Te [3]. Nevertheless, it was possible to confirm the chalcopyrite structure of LGT and measure its lattice constants and melting temperature (913 ± 10 K) [3]. Later we obtained yellow crystals of optical quality and updated the lattice parameters, measured dispersion of refractive indices and birefringence, analyzed phase matching conditions and estimated the nonlinear susceptibility [4,5]. Birefringence and nonlinear susceptibility of LGT are the highest among compounds of the $LiMeX_2$ family (0.094 and 42 pm/V respectively). Combined with large band gap (2.54 eV) this makes LGT promising for nonlinear applications in the mid-IR. The energy band structure and main output parameters such as refractive indices, birefringence and nonlinear optical coefficients were calculated from the first principles for LGT [6]. However, very little is known about its spectroscopic properties and the defects. In present paper we studied transmission and luminescence spectra and the band gap, as well as vibrational, Raman and IR absorption, spectra. Splitting of the LGT valence band was revealed and the effects due to crystal field and spin–orbit interaction were estimated. Since ^{6}Li interacts with thermal neutrons giving off charged particles with high energy (the $^6Li(n,\alpha)^3H$ reaction) LGT together with LISe may be promising for neutron detecting [7]: Thus its luminescent and counting parameters are also important.

2. Experimental

2.1. Crystal growth

LGT crystals were grown in a vertical two-zone furnace with a diaphragm using the Bridgman–Stockbarger technique. Temperature, at which crystallization started, was only several degrees lower than the melting temperature of the starting charge. LGT polycrystalline charge was synthesized in a glass carbon container. The elementary starting chemicals were of 99.99% purity for Li and 99.999% for Ga and Te. Composition of the starting charge differed from the stoichiometric one in order to provide the losses due to incongruent evaporation of Li and Te near the melting temperature and Li interaction with the container walls [4]. Li losses and melt dissociation result in deviations from stoichiometry in liquid phase

---

[*] Corresponding author.
E-mail address: eliseev.ap@mail.ru (A. Yelisseyev).

http://dx.doi.org/10.1016/j.optmat.2014.12.046
0925-3467/

and crystallization of several phases. Thus, growing from melt with essential Li deficit we obtained sometimes $LiGa_3Te_5$ crystals instead of $LiGaTe_2$. Hence the initial charge was taken rich in Li and Te. After starting charge loading into the ampoule, it was evacuated to a residual pressure of 10^{-3} torr and the components were alloyed for 4 h. The polycrystalline charge obtained was loaded in a dry camera into a silica ampoule with a layer of pyrolitic graphite on its inner surface. To prevent the dissociation free volume of the ampoule was filled with purified Ar. The sealed off ampoule was inserted then into the two-zone furnace for directed crystallization. In order to control the isotherm shape a forced heat sink from the lower part of the ampoule was arranged. The ampoule was heated slowly (for 16 h) till the whole content was melted at 940 ± 5 K and only a seed crystal in its initial part remained solid. Then the temperatures in both zones of the furnace were held fixed for one day. Afterwards the ampoule was shifted to the cold zone at a rate of 2–5 mm/day. As-grown or cleaved LGT crystals up to 4 mm in size have natural faces of complex shape and different color which varies from yellow to red and even black. We studied transparent yellow samples. LGT samples are less stable in air in comparison with other ternary lithium compounds such as LIS, LISe, LGS and LGSe, but natural or cleaved faces remain transparent for a long time if samples are kept in kerosene.

2.2. Crystal structure

Single crystal X-ray structural analysis showed that LGT crystallizes in chalcopyrite structure in contrast with other members of the $LiMeX_2$ family where Me = In, Ga and X = S, Se: the latter all have the wurtzite-type structure [8]. Lattice parameters of LGT are: $a = 6.3295(6)$ Å, $c = 11.682(1)$ Å, $V = 468.0(1)$ Å^3, and $Z = 4$, space group $I\bar{4}2d$, point group $\bar{4}2m$. Lattice parameters of single crystals are somewhat smaller then those of powders [3]. On the other hand, smaller lattice constants are typical of higher quality crystals [5]. Atomic coordinates and isotropic thermal parameters for LGT are given in Table 1.

In ideal tetragonal lattice of chalcopyrite the axial ratio is $c/a = 2.0$. However, because of difference in sizes of two types of cations there are two types of anion tetrahedrons. As a result crystal lattice has a tetragonal distortion, described by the δ parameter: $\delta = (1 - c/2a) \times 100\%$. The axial ratio $c/a \approx 1.85$ for LGT. According to the empirical rules established for such ternaries [1,2] this means that LGT will remain in the ordered chalcopyrite structure even at high temperatures. The axial ratio of a chalcopyrite is also a measure for the uniaxial tetragonal distortion from the underlying diamond-like face-centered cubic structure. This distortion is relatively large in LGT (7.7%) which results in substantial birefringence (0.094) and nonlinear coefficient (42 pm/V) [4].

2.3. Optical spectroscopy

Transmission spectra were recorded using a UV-2501PC Shimadzu spectrometer in the UV-to-near IR, whereas in the mid-IR we used a Bomem Fourier-Transform spectrometer. The photoluminescence (PL) spectra were measured using a SDL1 diffraction luminescence spectrometer with excitation from a 1 kW Xe lamp through MDR2 diffraction monochromator. PL spectra were measured usually at 80 and 300 K. For some wavelengths PL temperature dependence was measured in the 80–500 K range. The 50 mW diode lasers emitting at 405 and 532 nm and a 100 W Hg lamp were used also for excitation.

Table 1
Atomic coordinates and isotropic thermal parameters U_{iso}.

Atom	x	y	z	U_{iso} (Å^2)
Li	0	0	0	0.026(9)
Ga	0.5	0	0.25	0.014(1)
Te	0.2666(1)	0.75	0.125	0.016(1)

3. Results and discussion

3.1. Transmission

Yellow LGT samples transmit in the 0.525–16 μm on the $Tr = 1\%$ level but the clear transparency region with $Tr > 60\%$ extends from 2.5 to 12 μm (Fig. 2). Some losses take place at shorter wavelengths: they are due both to absorption of point defects and Raileigh light scattering on inclusions of side phases in crystal bulk. Light scattering is maximal at short wavelengths and decreases as $1/\lambda^4$ as wavelength grows. An intense absorption band centered near 16 μm with a shoulder near 19 μm can be observed in the transmission spectrum of LGT and more clearly in the absorption coefficient (Fig. 2). This band serves as an upper limit for practical optical applications. For the band-gap measurements a thin ($d \approx 250$ μm) yellow plate of LGT with natural faces was used. The fundamental absorption edge was measured at 11 different temperatures from 80 to 325 K. At short wavelengths the recorded curves can be approximated with straight lines in the coordinates $(\alpha \times h\nu)^2 = f(h\nu)$, where α is the absorption coefficient in cm^{-1} and $h\nu$ is the photon energy in eV (Fig. 3). This means that fundamental absorption edge is due to direct allowed electronic transitions and band gap value E_g can be determined from the cross points between the straight lines and the abscissa axis [9]. In the insert of Fig. 3 the band gap values are plotted versus temperature T. The band gap values are 2.65 and 2.41 eV at 80 and 300 K, respectively. E_g depends linearly on temperature and $dE_g/dT = 1.106 \times 10^{-3}$ eV/K. E_g(LGT) is substantially larger than the predictions of Ref. [2] (1.7 eV). It is interesting to note that E_g(LGT) substantially exceeds also the band-gap value known for the isostructural $AgGaTe_2$ (1.316 eV) [10].

3.2. Vibrational spectra

Raman spectrum for $LiGaTe_2$ in two different scales and a fragment of IR absorption spectrum are given in Fig. 4. For a chalcopyrite-type structure with the space group $I\bar{4}2d$ the symmetry of the crystal decomposes the optical vibrational modes into 15 normal modes $A_1 + 2A_2 + 3B_1 + 3B_2 + 6E$ [11], where B_2 and E are polar Raman active modes with transverse optical (TO) and longitudinal optical (LO) modes, A_1 and B_1 are nonpolar Raman active modes, and A_2 is an optically inactive mode. The B_2 and E vibrational modes are IR active and associated with anions and cations [11,12].

Four groups of peaks can be seen in the Raman spectra (Fig. 4). The dominating A_1 peak at 120.0 cm^{-1}, related to purely anionic (Te) vibrations, exhibits a shoulder at 141.6 cm^{-1}. The same A_1 mode is located near 122 cm^{-1} in $LiInTe_2$ [3]. Its frequency is inversely proportional to the square root of the anion atomic weight [12] and according to Ref. [11] also inversely proportional to the square root of the cation mean atomic weight. The first dependence seems to be fulfilled if we compare with $LiGaS_2$ and $LiGaSe_2$ [13]. Although these related lithium compounds have β-$NaFeO_2$ (wurtzite-type) structure, a similar dominating line with A_1 symmetry is observed there, too [3]. The second dependence can be checked by comparison with the A_1 modes of $LiInTe_2$ [3] and $AgGaTe_2$ [11]. It is not fulfilled which can be attributed to the different binding nature of the Li-containing chalcopyrites: the Li atoms are rather weakly bound to the Te atoms here [14].

The low frequency vibrations are characterized by a strong line at 77.8 cm^{-1} (similar to one observed in $LiInTe_2$ [3]) with a weaker 75.7 cm^{-1} peak seen as shoulder in Fig. 4. Two groups of lines are observed at higher frequencies. The first group near 200 cm^{-1} consists of peaks at 196.8, 202.2, 211.8 and 221.4 cm^{-1}. In the second